Supplementary Information

Homogeneous immunoassay for cyclopiazonic acid based upon mimotopes and upconversion-resonance energy transfer

Fernando Pradanas-González[a], Riikka Peltomaa[b], Satu Lahtinen[b], Álvaro Luque-Uría[a], Vicente Más[c], Rodrigo Barderas[c], Chris M. Maragos[d], Ángeles Canales[e], Tero Soukka[b]*, Elena Benito-Peña[a]*, María C. Moreno-Bondi[a]†

[a] Department of Analytical Chemistry, Faculty of Chemistry, Complutense University of Madrid, Ciudad Universitaria, 28040 Madrid, Spain.
[b] Department of Life Technologies/Biotechnology, University of Turku, Kiinamyllynkatu 10, 20520 Turku, Finland.
[c] Instituto de Salud Carlos III, Ctra. Majadahonda-Pozuelo, 28220 Madrid, Spain.
[d] Mycotoxin Prevention and Applied Microbiology Research Unit, National Center for Agricultural Utilization Research, Agricultural Research Service, USDA, 1815 N University, Peoria, IL 61604, USA.
[e] Department of Organic Chemistry, Faculty of Chemistry, Complutense University of Madrid, Ciudad Universitaria, 28040 Madrid, Spain.
†*The late*.

Contents

Experimental

Phage-based ELISA

Individual phage-displayed peptides were tested in different ELISAs to select clones that specifically bind to the mAb-1418. Direct phage-based ELISA was performed by coating MaxiSorp 96-well microtiter plates with 200 ng of mAb-1418 in 60 µL of 0.1 M sodium bicarbonate buffer, pH 8.6, during an overnight incubation at +4°C. The wells were then rinsed three times with PBS-T (0.05% v/v) and blocked with 3 % (w/v) BSA in PBS (pH 7.4) for 2 h at RT. After another washing step under the same conditions, 60 µL/well of the amplified monoclonal phages were added to the mAb-coated wells in a 1:20 dilution (in PBS with 0.05% (v/v) Tween-20 and 0.1% (w/v) BSA) and incubated for 1h at RT with slow shaking. Unbound phages were removed by a further washing step and then 60 µL/well of anti-M13-HRP (in a 1:2000 dilution in PBS with 0.05% (v/v) Tween-20 and 0.1% (w/v) BSA) were added and allowed to bind to the bound phages for 1 h. The plate was rinsed again three times with PBS-T (0.05% v/v) and the enzymatic reaction took place by adding 60 µL of TMB substrate solution to each well. The reaction was stopped after a few seconds with 60 µL of 2 M H_2SO_4, and the analytical signal was obtained by measuring the absorbance at 450 nm with a CLARIOstar microplate reader from BMG (Ortenberg, Germany). Positive clones were successively assayed in phage-based competitive ELISA following the protocol described above but adding the phage dilutions together with 100 ng mL^{-1} CPA to assess the competition, or with variable concentrations of CPA (range from 0 to 10 ng mL^{-1}) for the calibration plots.

Synthetic peptide-based ELISA

For the development of phage-free competitive immunoassays, the four peptide sequences were chemically synthetized and conjugated to biotin by Peptide Synthetics with the sequence $AC(X)_7C$-GGGSK(Biotin)-NH_2. A disulfide bond between the two cysteines allowed the mimotope to obtain a constrained loop shape in an analogous way as presented in the phage library. The same GGGS linker that was included in the phage-displayed form was added, and biotin was included on the side chain of the lysine residue.

For the heterogeneous synthetic peptide-based ELISA, all the incubations were carried out in PBS with 0.05% (v/v) Tween-20 and 0.1% (w/v) BSA at room temperature with slow shaking and, after each incubation step, a washing step consisting of three rinses with PBS-T (0.05%, v/v) was performed. In order to ensure an effective coating of the neutravidin magnetic beads with the synthetic mimotope, different amounts (5–50 ng/well in 100 µL) were tested in the absence and the presence of CPA (**Fig. S13),** and 5 ng/well of the synthetic peptide was selected to construct additional calibration curves. Briefly, MaxiSorp 96-well microtiter plates were blocked with 3% (w/v) BSA for 1h. After the blocking step, 5 µg (in 20 µL) of neutravidin-coated magnetic beads were incubated with 5 ng (in 100 µL) of biotinylated mimotope for 30 min. Then, 100 µL of different solutions containing 0.5 µg mL^{-1} of mAb-1418 and varying concentrations of CPA (0−50 ng mL^{-1}) were added to the wells and incubated for another 30 min. Finally, a 1:2000 dilution

of rabbit anti-mouse-HRP solution was added and incubated 30 min. TMB substrate (60 µL) was added to each well and the enzymatic reaction was stopped with 60 µL of 2 M H_2SO_4. The absorbance was measured with a CLARIOstar microplate reader.

Conjugation of UCNPs with streptavidin

UCNPs ($NaYF_4$:Yb^{3+}, Er^{3+}) were synthesized (Palo et al., 2017) and surface-modified with poly(acrylic acid) (PAA) (Raiko et al., 2021). The functionalized UCNP-PAA were conjugated to streptavidin (SA) following the approach described for the conjugation of other macromolecules with some modifications (Raiko et al., 2021). Briefly, 2 mg of UCNP-PAA were activated for 45 min using EDC/sulfo-NHS chemistry (20 mM and 30 nM, respectively) in 260 µL of 20 nM 2-(N-morpholino) ethanesulfonic acid (MES) buffer (pH 6.1). The particles were centrifuged and rinsed with MES buffer to remove the remaining ECD/sulfo-NHS. The activated UCNP-PAA were incubated with 0.4 mg of SA for 2.5 h at room temperature in 250 µL of 20 mM MES buffer (final concentrations 8 mg mL^{-1} and 1.6 mg mL^{-1}, respectively). The reaction was stopped by blocking the surface with a 2 M asymmetric dimethylarginine (ADMA) solution for 30 min (final concentration 50 mM) and the UCNP(PAA)-SA were washed twice with 10 mM Tris (pH 8), 0.1 % Tween-20. Finally, the SA-conjugated nanoparticles were resuspended in 250 µl of SA storage buffer composed of 5 mM Tris (pH 8), 0.2% Tween-85, 0.05% NaN_3 and stored at +4 °C.

The success of the bioconjugation was tested in a biotin-based competitive assay (Rantanen et al., 2007). Briefly, 7.5 µg mL^{-1} of UCNPs-SA were mixed with different concentrations of biotin-Alexa Fluor 555 (bio-AF555) (0.5-32 nM) in the absence and the presence of free biotin (5 µM) in a total volume of 80 µL in the assay buffer. After 30 min of incubation, the emission of AF555 (measured during the excitation, 2-second excitation pulse) was measured at 600 nm upon excitation of the UCNPs in the near-infrared (975 nm), in modified Plate Chameleon microplate reader.

Fab anti-CPA conjugation to fluorophore AF555

The conjugation of the Fab(anti-CPA) to the fluorophore Alexa Fluor 555 (AF555) was performed according to a protocol described before with slight changes (Akter and Lamminmäki, 2021). Briefly, 188 µg Fab(anti-CPA) were incubated with a 15-fold molar excess of Alexa Fluor 555 (AF555) succinimidyl ester in a total volume of 250 µL in 100 mM sodium carbonate buffer pH 9.3 for 1 h at room temperature. The labelled antibody was double-purified by molecular exclusion chromatography using NAP-5 and NAP-10 columns.

The concentration of the labeled Fab was obtained according to manufacturer's instructions as ($A_{280}-A_{555}$ × 0.08)/70000) (M) where 0.08 is the correction factor for the absorption of the fluorophore at 280 nm and 70000 is the approximate molar extinction coefficient ($cm^{-1}\,M^{-1}$) of the Fab. The labeling degrees were calculated as follows: A_{555}/[150000 × protein concentration (M)], where 150000 is the approximate molar extinction coefficient ($cm^{-1}\,M^{-1}$) of AF555 at 550 nm.

NMR interaction study

The mimotope A2–antibody interaction was confirmed by using NMR as previously described (Peltomaa et al., 2020).

SPR measurements

The binding kinetics of the biotinylated synthetic mimotopes or CPA, as toxin-conjugate CPA-β-lactoglobulin (Maragos et al., 2017) (CPA-BLG), with the target anti-CPA antibody mAb-1418 were determined by surface plasmon resonance (SPR) analysis on BIAcore T-200 (Cytiva, Chicago, IL, USA) at +25°C. Carboxymethylated dextran surfaces of Sensor Chips CM5 Series S (Cytiva) were activated with EDC/NHS to covalently immobilize different antibody ligands. After the modification of the surfaces, 1 M ethanolamine was injected in order to block the remaining active sites on the chips.

For the biotinylated synthetic mimotopes, an anti-biotin IgG (ligand, 100 µg mL^{-1} in 10 mM sodium acetate pH 5.0, flow rate 5 µL min^{-1}, 540 s) was selected to be covalently immobilized to the activated surface of the chip, in both control and sample channels, with approximately 7000 response units (RU). The biotinylated synthetic mimotopes (20 ng mL^{-1}) diluted in the running buffer (10 mM phosphate buffer saline with 0.05% (v/v) Tween-20) was injected at a flow rate of 5 µL min^{-1} for 40 s in the sample channel achieving a response of approximately 6 RU. Thereafter, different concentrations of the anti-CPA mAb-1418 (0−4 µM) were injected at a flow rate of 30 µL min^{-1} for 120 s contact time and 60 s dissociation time, in both control and sample channels. For the regeneration of the chip surface between cycles, 10 mM glycine-HCl (pH 1.7) was added at a flow rate of 30 µL min^{-1} for 150 s.

For the CPA-BLG, an anti-mouse IgG (ligand, 30 µg mL^{-1} in 10 mM sodium acetate pH 5.0, flow rate 5 µL min^{-1}, 420 s) was selected to be covalently immobilized to the activated surface of the chip, in both control and sample channels, obtaining a response of approximately 6000 RU. The anti-CPA mAb1418 (10 µg mL^{-1}) diluted in the running buffer was injected at a flow rate of 10 µL min^{-1} for 150 s in the sample channel achieving a response of approximately 700 RU. Then, different concentrations of the CPA-BLG conjugate (0−31 nM) were injected at a flow rate of 60 µL min^{-1} for 300 s contact time and 400 s dissociation time, in both control and sample channels. For the regeneration of the chip surface between cycles, 10 mM glycine-HCl (pH 1.7) was added at a flow rate of 30 µL min^{-1} for 100 s.

HPLC-DAD methodology

The immunoassay was validated by high performance liquid chromatography (HPLC) coupled to a diode array detector (DAD) from Agilent Technologies (1200 series). Reversed-phase chromatography was performed on a Zorbax SB-C18 (3.5 µm x 4.6 mm x 150 mm) chromatographic column (from Agilent Technologies) and CPA was eluted under isocratic conditions by using aqueous 0.1% trifluoroacetic acid solution (solvent A) and MeCN supplemented with 0.1% trifluoroacetic acid (solvent B) in a 30:70 ratio

(v/v). The injection volume was 100 µL and the analyte was monitored at 282 nm. The quantification was carried out by external standard calibration with matrix-matched calibration curves.

Results

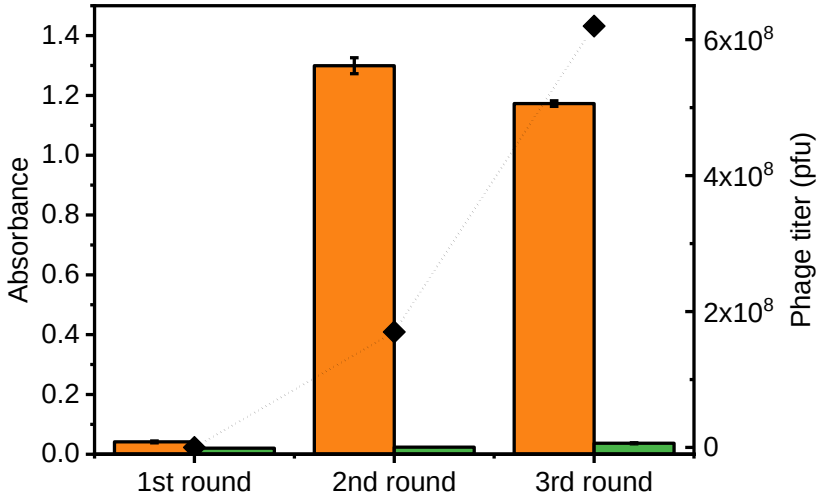

Figure S1. Phage titer and polyclonal ELISA.

Black diamonds show the phage titer over the rounds (right y-axis), and the bars represent the results of the Phage-based ELISA with polyclonal phages after three panning rounds for CPA peptide mimetics. A higher binding was observed towards the mAb-1418 monoclonal antibody (orange) in comparison to background wells (green) for the second and third rounds. The phage concentration evaluated in all rounds was 5×10^9 pfu mL^{-1}. The ELISA results are shown as the mean values of the absorbance ± the standard deviation of the mean (*n* = *3*).

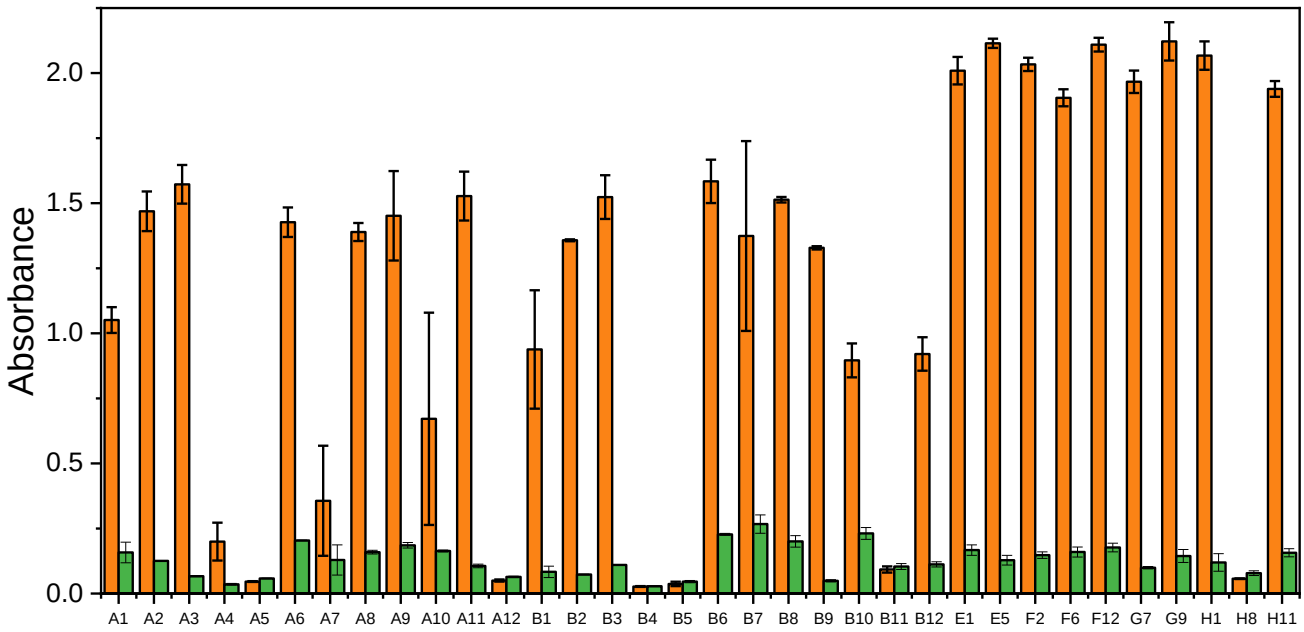

Figure S2. Monoclonal phage-based ELISAs with individual clones.

Phase-based ELISA with the 34 individual phage clones selected from rounds 2 and 3. The vast majority of the clones presented specificity towards the target wells (orange) and negligible signal for background wells without the antibody (green). The phage dilution evaluated in all rounds was 1:20 from the stocks. The results are shown as the mean values of the absorbance ± the standard deviation of the mean (*n* = *3*).

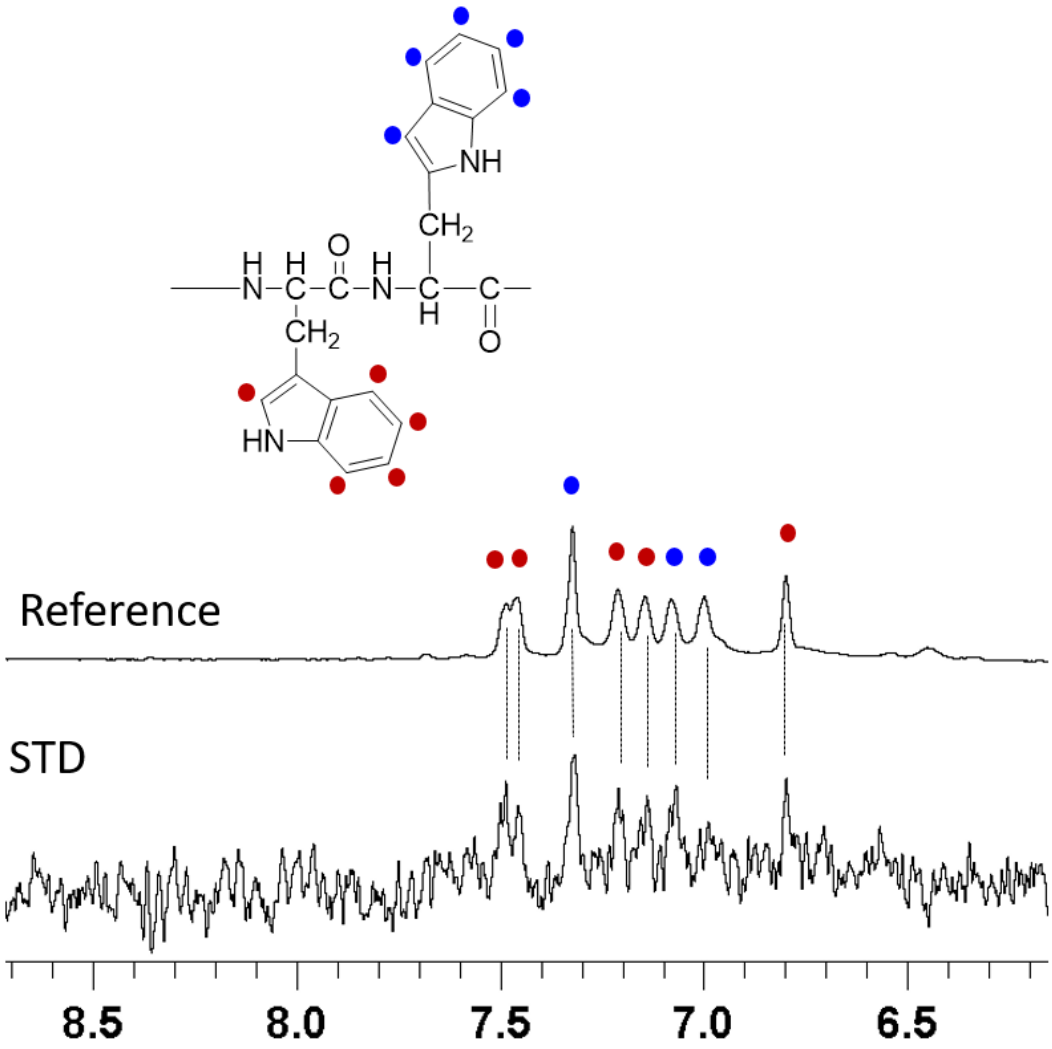

Figure S3. Mimotope A2–antibody interaction by using NMR.

The biotinylated ACNWWDLTLC (peptide A2)–antibody interaction was confirmed by using NMR as previously described (Peltomaa et al., 2020). The STD experiment was acquired with 3k scans on a 700 MHz Bruker spectrometer equipped with a cryoprobe. The peptide concentration was 300 mM and the peptide:antibody ratio 60:1. The off resonance frequency and on resonance frequencies were 100 ppm and -1 ppm, respectively. STD spectrum displays the aromatic signals of both tryptophans pointing out that both are interacting with the antibody.

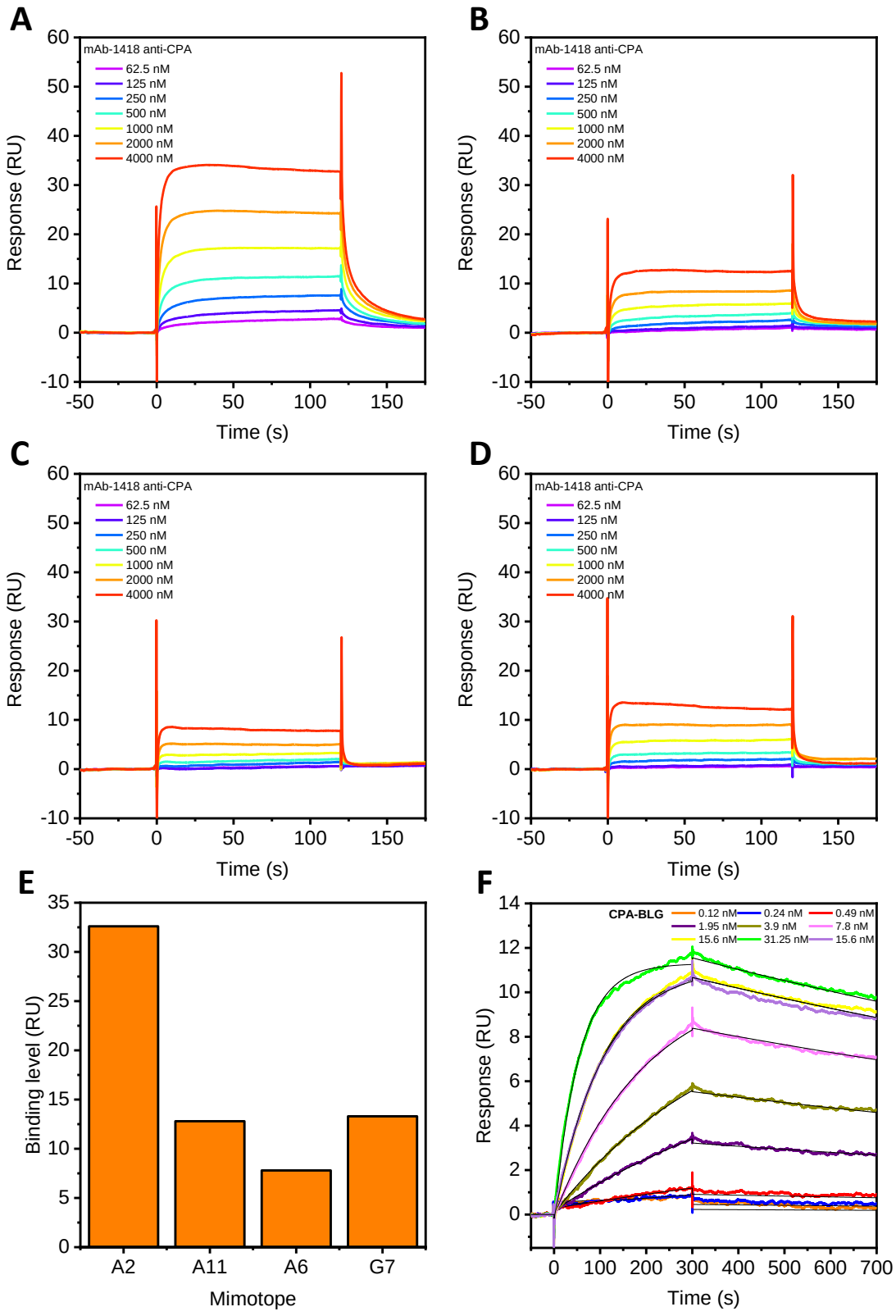

Figure S4. SPR measurements.

Kinetic analyses of different biotinylated synthetic mimotopes by surface plasmon resonance (SPR). (A) A2-biotin, (B) A11-biotin, (C) A6-biotin and (D) G7-biotin were captured with an anti-biotin IgG and the mAb-1418 was passed through the chip surface as the analyte (0 −4 μM). (E) Binding level of the mimotopes at 4 μM mAb-1418. (F) Binding of CPA-BLG (0 −31 nM) to the immobilized mAb-1418. Sensorgrams corresponding to the antibody−CPA-BLG kinetics were fitted to a 1:1 binding model.

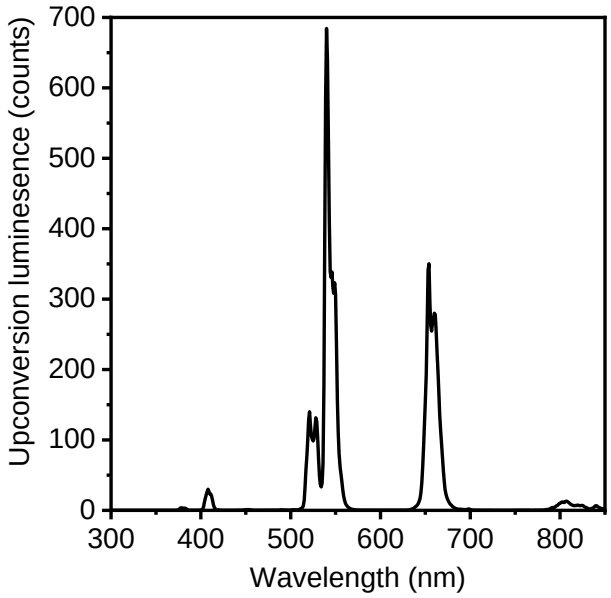

Figure S5. Emission spectrum of UCNPs.

Emission spectrum of $NaYF_4$:Yb^{3+}, Er^{3+} UCNPs. The spectrum was measured with Cary Eclipse fluorescence spectrophotometer (Agilent Technologies). For the measurement, the device was equipped with 980 nm laser diode (λ_{emi} = 980 nm).

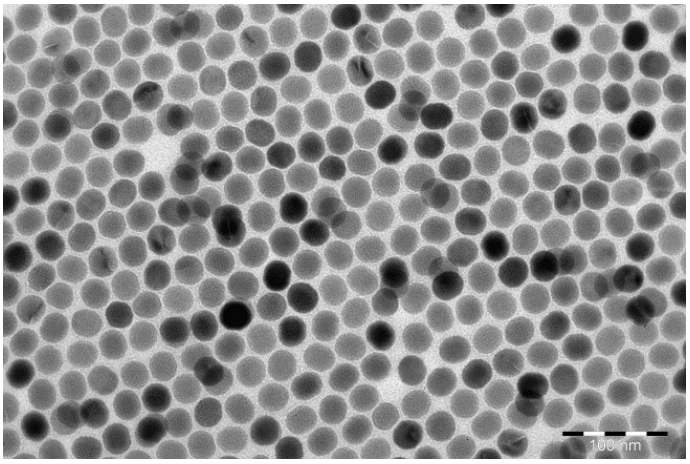

Figure S6. TEM image of UCNPs.

Transmission electron microscopy (TEM) image of $NaYF_4$:Yb^{3+}, Er^{3+} UCNPs (80 000 magnification). The nanoparticles were imaged with JEM-1400 Plus TEM using 80 kV electron beam. According to the image, the particle size was 27.3 nm with a standard deviation around 1 nm (number of particles counted 100).

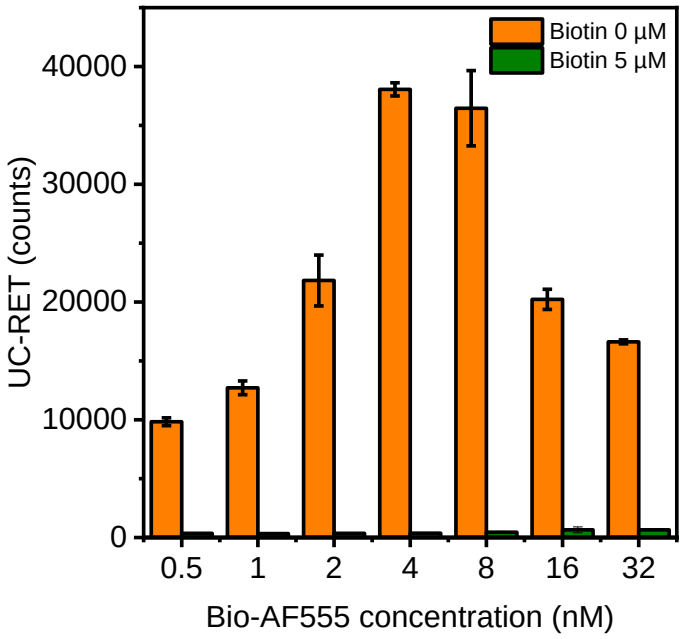

Figure S7. UCNP-SA test in a biotin-based assay.

Biotin-based competitive assay for testing the correct functionalization of UCNPs with streptavidin (7.5 µg mL^{-1}). Different concentrations of biotin-AF555 were assayed in the absence and the presence of free biotin (5 µM) to control the dependence of the signal on the binding of biotin-AF555 to streptavidin on the UCNP surface. The results are shown as the average fluorescence values ± the standard deviation of the mean (*n* = 3).

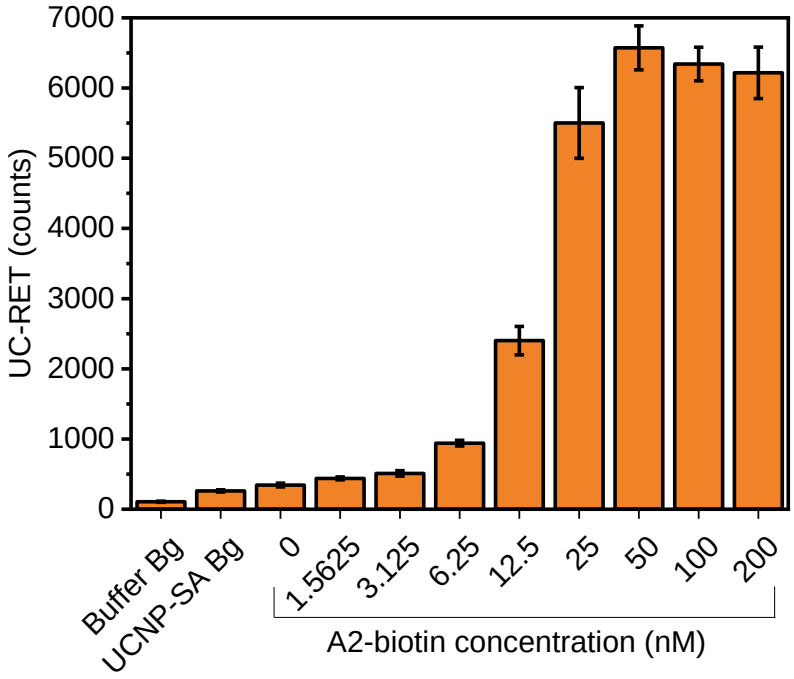

Figure S8. A2-biotin titration for the UC-RET-based assay.

A2-biotin concentration was optimized (1.5625–200 nM) for a given concentration of UCNP-SA (7.5 µg mL^{-1}) and Fab-AF555 (16 nM). The highest signals were obtained with 50 nM A2-biotin. The results are shown as the average fluorescence values ± the standard deviation of the mean (*n* = 3).

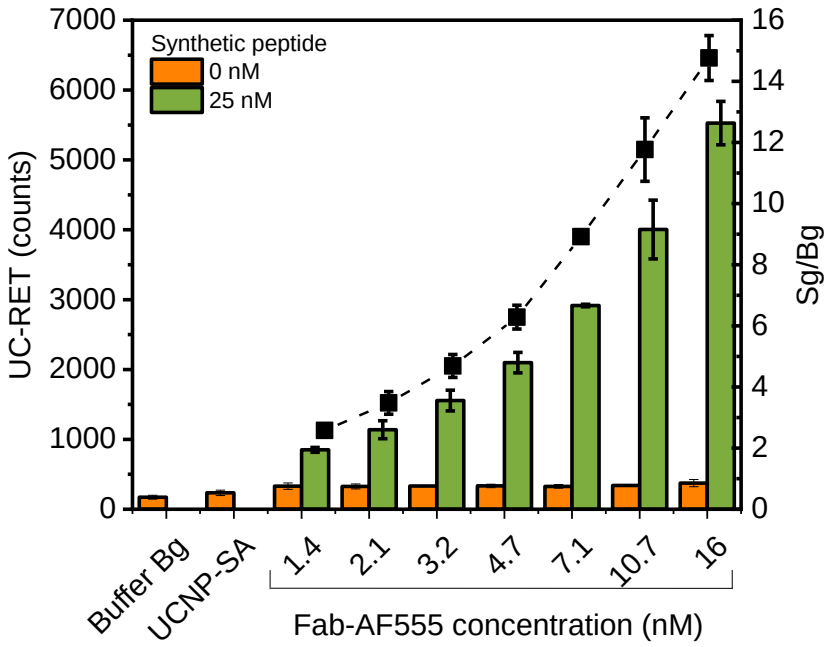

Figure S9. Effect of Fab-AF555 concentration on the assay.

Evaluation of the effect of the Fab-AF555 concentration on fluorescence signals and signal-to-background (Sg/Bg, black squares) ratios of the immunoassay (A2-biotin 25 nM and UCNP-SA 7.5 µg mL^{-1}). The results are shown as the average fluorescence values ± the standard deviation of the mean (*n* = 3).

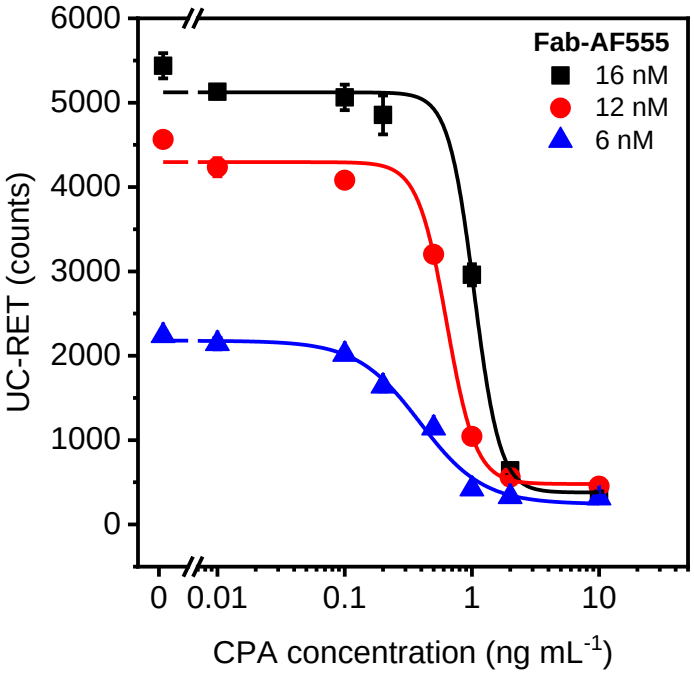

Figure S10. Sensitivity of the assay with different concentrations of Fab-AF555.

Evaluation of the sensitivity of the assay with different concentrations of Fab-AF555 (A2-biotin 25 nM and UCNP-SA 7.5 µg mL^{-1}). The results are shown as the average fluorescence values ± the standard deviation of the mean (*n* = 3).

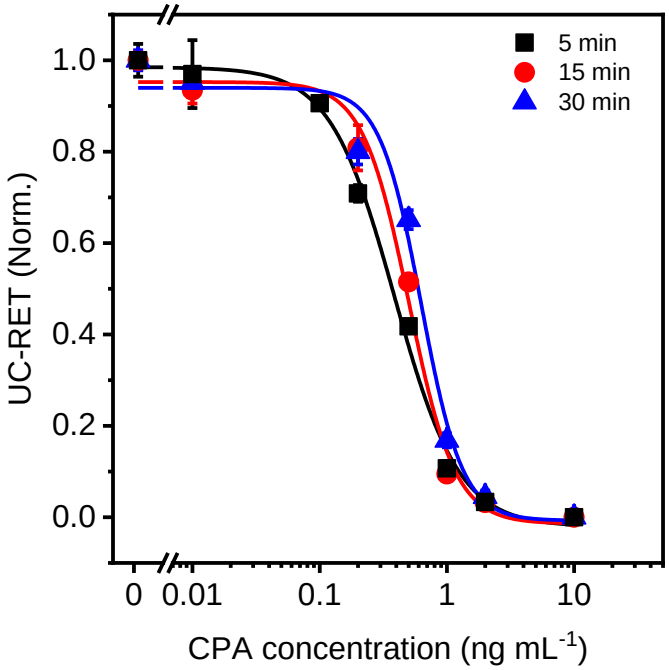

Figure S11. Evaluation of incubation time in the 1-step assay.

Evaluation of the incubation time in the 1-step assay. The results are shown as the normalized signals values ± the standard deviation of the mean (*n* = 3).

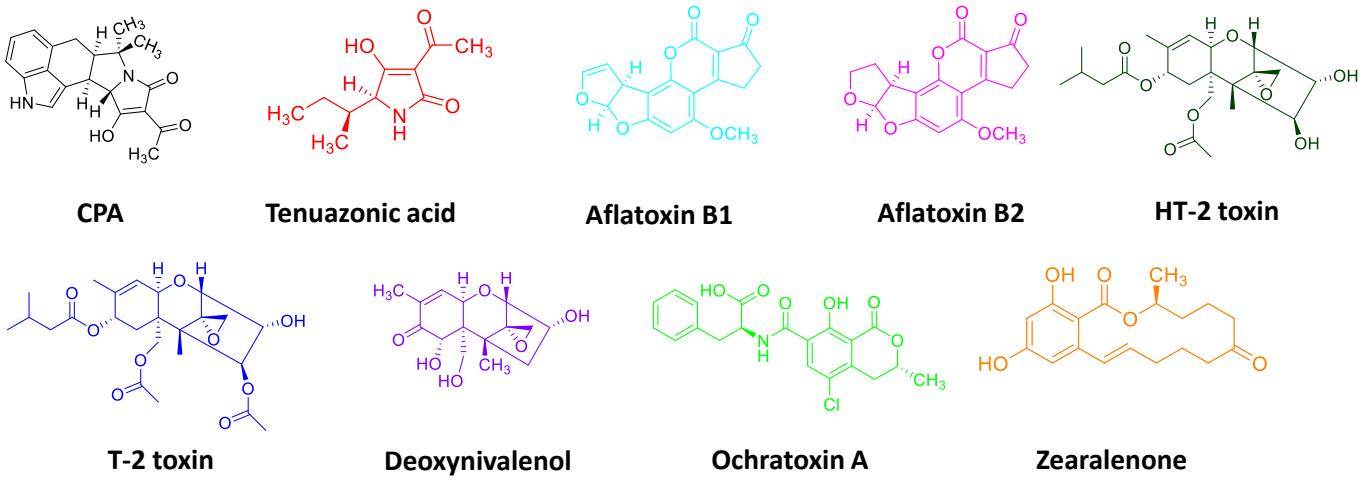

Figure S12. Mycotoxin structures.

Chemical structures of cyclopiazonic acid (CPA) and mycotoxins tested in cross-reactivity studies.

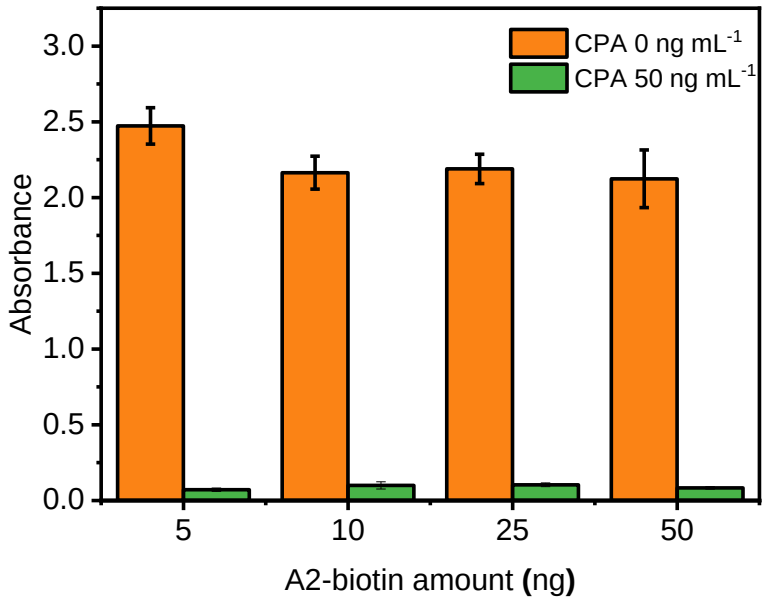

Figure S13. A2-biotin saturation coating for phage-free based ELISA.

Optimization of the amount of the biotinylated synthetic mimotope (A2-biotin) for the implementation of the phage-free based ELISA. Different amounts of A2-biotin were assayed in combination with 5 µg of neutravidin-coated magnetic beads and 0.5 µg mL^{-1} of mAb-1418 in the absence and the presence of 50 ng mL^{-1} CPA to control the specificity of the antibody binding to the mimotope. The results are shown as the average absorbance values ± the standard deviation of the mean (n = 3).

Table S1. Analytical features comparison of the four mimotopes (named A2, A6, A11, and G7) in both phage-based and synthetic peptide-based ELISAs for CPA.

	Phage-based ELISA				Synthetic peptide-based ELISA			
	A2	**A6**	**A11**	**G7**	**A2**	**A6**	**A11**	**G7**
LOD (ng mL^{-1})	0.34	0.34	0.33	0.40	0.42	0.41	0.42	0.44
IC_{50} (ng mL^{-1})	0.58	0.61	0.57	0.62	0.89	0.87	0.86	0.91
Dynamic range (ng mL^{-1})	0.42−0.81	0.42−0.88	0.40−0.81	0.44−0.82	0.56−1.41	0.54−1.37	0.54−1.35	0.57−1.43

Table S2. Comparison of the analytical features of the assays developed in this work with other reported immunoassays for CPA in maize samples.

Immunoassay	Format	Detection time	IC_{50} (ng mL^{-1})	Working range[d] (ng mL^{-1})	LOD (ng mL^{-1})	LOD (µg kg^{-1})	Ref.
ELISA	Heterogeneous	O/N[a] + 1 h 45 min	0.42 – 0.93	*n.d.*	0.08–0.3	100	(Yu and Chu, 1998)
ELISA	Heterogeneous	O/N[a] + 3 h	1.1	0.24–1.39	*n.d.*	< 2	(Maragos et al., 2017)
iSPR	Heterogeneous	> 10 min[b]	0.84	*n.d.*	0.45	17	(Hossain et al., 2019)
ELISA	Heterogeneous	5 h 15 min	0.4	0.15–1.3	0.2	*n.d.*	(Li et al., 2020)
LFIA	Heterogeneous	> 2 h[c]	*n.d.*	*n.d.*	*n.d.*	2.5	
Phage-based ELISA	Heterogeneous	O/N[a] + 4 h	0.58	0.42–0.81	0.34	*n.d.*	This work
Synthetic peptide-based ELISA	Heterogeneous	2 h 30 min	0.89	0.56–1.41	0.42	*n.d.*	
UC-RET	Homogeneous	5 min	0.36	0.15–0.9	0.03	1.5	

ELISA: enzyme-linked immunosorbent assay; iSPR: imaging surface plasmon resonance; LFIA: lateral flow immunoassay; *n.d.*: not determined; UC-RET: upconversion-resonance energy transfer. ([a]) O/N: overnight incubation of the antibody or CPA-conjugate. ([b]) More than 10 min per SPR cycle including association step, amplification step with secondary antibody and regeneration step. ([c]) Including preparation of the strip. ([d]) Working range as IC_{20} to IC_{80} inhibition.

References

Akter, S., Lamminmäki, U., 2021. Anal. Bioanal. Chem. 413, 6159–6170.

Hossain, Z., Busman, M., Maragos, C.M., 2019. Anal. Bioanal. Chem. 411, 3543–3552.

Li, Y., Liu, L., Kuang, H., Xu, C., 2020. J. Food Sci. 85, 105–113.

Maragos, C.M., Sieve, K.K., Bobell, J., 2017. Mycotoxin Res. 33, 157–165.

Palo, E., Tuomisto, M., Hyppänen, I., Swart, H.C., Hölsä, J., Soukka, T., Lastusaari, M., 2017. J. Lumin. 185, 125–131.

Raiko, K., Lyytikäinen, A., Ekman, M., Nokelainen, A., Lahtinen, S., Soukka, T., 2021. Clin. Chim. Acta 523, 380–385.

Rantanen, T., Päkkilä, H., Jämsen, L., Kuningas, K., Ukonaho, T., Lövgren, T., Soukka, T., 2007. Anal. Chem. 79, 6312–6318.

Yu, W., Chu, F.S., 1998. J. Agric. Food Chem. 46, 1012–1017.

Peltomaa, R., Farka, Z., Mickert, M.J., Brandmeier, J.C., Pastucha, M., Hlaváček, A., Martínez-Orts, M., Canales, Á., Skládal, P., Benito-Peña, E., Moreno-Bondi, M.C., Gorris, H.H., 2020. Biosens. Bioelectron. 170, 112683.